FULL PAPER
THE ANALYST
www.rsc.org/analyst

Micro-machined planar field asymmetric ion mobility spectrometer as a gas chromatographic detector

G. A. Eiceman,*[a] E. G. Nazarov,[a] R. A. Miller,[b] E. V. Krylov[a] and A. M. Zapata[c]

[a] *Department of Chemistry and Biochemistry, New Mexico State University, Las Cruces, NM 88003, USA*
[b] *Sionex Corporation, Wellesley Hills, MA 02481, USA*
[c] *Draper Laboratory, Cambridge, MA, USA*

Received 18th December 2001, Accepted 1st March 2002
First published as an Advance Article on the web 20th March 2002

A planar high field asymmetric waveform ion mobility spectrometer (PFAIMS) with a micro-machined drift tube was characterized as a detector for capillary gas chromatography. The performance of the PFAIMS was compared directly to that of a flame ionization detector (FID) for the separation of a ketone mixture from butanone to decanone. Effluent from the column was continuously sampled by the detector and mobility scans could be obtained throughout the chromatographic analysis providing chemical information in mobility scans orthogonal to retention time. Limits of detection were approximately 1 ng for measurement of positive ions and were comparable or slightly better than those for the FID. Direct comparison of calibration curves for the FAIMS and the FID was possible over four orders of magnitude with a semi-log plot. The concentration dependence of the PFAIMS mobility scans showed the dependence between ion intensity and ion clustering, evident in other mobility spectrometers and atmospheric pressure ionization technologies. Ions were identified using mass spectrometry as the protonated monomer and the proton bound dimer of the ketones. Residence time for column effluent in the PFAIMS was calculated as ~1 ms and a 36% increase in extra-column broadening *versus* the FID occurred with the PFAIMS.

Introduction

Detectors in gas chromatographic separations have long supplemented the chromatographic performance of columns by providing additional information related to a sample. These may be either enhanced selectivity of sample ionization (electron capture detector, surface ionization detector) or additional chemical–structural information about a component of a sample (mass selective detector).[1–3] Though a remarkably high level of column efficiency can be obtained with commercially available bonded-phase capillary columns, the widespread utilization of mass spectrometers as a GC detector in environmental, industrial, and medical measurements is evidence that additional dimensions of information in GC separations have importance. Thus, plots of ion abundance *versus m/z* orthogonal to retention time often add analytical confidence sufficient to justify the high costs of purchase, operation, and maintenance of mass spectrometers as GC detectors.

In 1982, a conventional IMS drift tube design was described for use as a GC detector for capillary columns, where sample clearance in the source region was fast and sample neutrals were prevented from diffusing into the drift region.[4] This detector exhibited high-speed response, low memory effects and reproducible gas phase ion chemistry inside the drift tube. Recently, class specific information has been discovered in mobility spectra under certain conditions of low moisture and high temperature.[5,6] Consequently, mobility spectrometers can be adjusted to provide spectra either with intact product ions or with fragment ions so that information density might be controlled by the analyst. In such conditions, confidence levels in categorizing mobility spectra by chemical class may be very high (for chemicals class 90–95%, for chemical identification inside classes ~80%). In summary, the information density in mobility spectra is sufficiently high so that mobility spectrometers may be considered economical and sensible alternatives to a mass spectrometer as GC detectors when utilities, size, weight and cost are restrictions. One example is air quality monitoring on-board the international space station where measurements are now made using a GC/IMS instrument, the Volatile Organic Analyzer.[7]

A significant limitation to the widespread use of the conventional mobility spectrometers as GC detectors has been the cost of manufacturing drift tubes. Compared to mass spectrometers, mobility spectrometers are simple and inexpensive; however, traditional mobility detectors can be considered costly compared with the FID or a thermal conductivity detector. Though miniaturization of drift tubes may be helpful in reducing costs of manufacture of mobility spectrometers,[8] the best route to low cost detectors could be a combination between miniaturization and methods of mass production. A drift tube that may be regarded as economical has been described and is a planar micro-machined drift tube[9–11] with rectangular dimensions of 25 mm long × 0.5 mm deep × 5 mm wide. This drift tube was operated using a non-traditional approach with high field asymmetric waveform dependent mobility methods.[12,13] Though the drift tube is small and ion losses to the walls might be considered a complication, sub-nanogram detection limits were obtained in the absence of ion shutters. Since these drift tubes are manufactured using mass fabrication methods, the most expensive part of the IMS analyzers, the drift tubes, now can be made in mass with concomitant low costs. The size of the analyzer and supporting electronics suggest that this design may be attractive especially for field gas chromatographs and process analyzers.

In a high field asymmetric waveform-operated drift tube, ions are transported through the drift tube by a gas flow and electric fields are applied perpendicular to the ion transport through a planar drift region.[12,13] Unlike the behavior of ions in traditional drift tubes, ion separation in this drift tube occurs according to the ion mobility dependence on the electric field intensity. The small size of the miniature mobility analyzer allows ion residence times of about 1 ms and consequently the scan time

 DOI: 10.1039/b111547m

for an entire spectrum can be less than 1 s. This makes the speed of ion characterization comparable to that of a quadrupole mass spectrometer, except that unlike a mass spectrometer, this drift tube functions at atmosphere pressure (the resolution of these drift tubes resembles that of early quadrupoles, not contemporary designs). Nonetheless, an opportunity may exist with these drift tubes to provide a gas chromatographic detector where retention time is supplemented with orthogonal information obtained as a continuous record of mobility scans from the FAIMS throughout a GC analysis.

In a preliminary assessment of a micro-machined PFAIMS drift tube as a GC detector,[9] the limits of detection were found to be about 50 pg and orthogonal information was provided in mobility scans for oxygen containing volatile organic compounds. A thorough comparison with a standard detector for GC, however, was not completed, making a comparative assessment of the detector difficult, particularly with regard to extra column broadening. The objective of this work has been to compare directly and quantitatively the analytical performance a micro-machined PFAIMS as a GC detector with that of a commercially available FID. The comparison is performed through parallel studies with identical samples, column, and chromatograph. A homologous series of ketones with carbon numbers from 4 to 9 was chosen for evaluation owing to the properties of ketones in traditional mobility spectrometers. Ketones exhibit comparatively high proton affinities leading to the formation of protonated monomers and proton bound dimers with structures of the kind $MH^+(H_2O)_n$ and $M_2H^+(H_2O)_n$, respectively. The concentration dependence and mobility of homogeneous and heterogeneous cluster ions for ketones have been well-described.[14] Moreover, the thermal stability of these cluster ions is strong without fragmentation or substantial declustering below 200 °C. In the studies below, the concentration dependence of the orthogonal information in a high field drift tube, available as mobility scans, has been evaluated and is reported for the first time.

Experimental

Instrumentation

A model 5880 gas chromatograph (Hewlett-Packard Co., Avondale, PA) was equipped with an HP splitless injector, 25 m SP 2300 capillary column (Supelco, Bellefonte, PA), a flame ionization detector, and a micro-machined PFAIMS analyzer as a detector.[9–11] The carrier gas was nitrogen (99.99%) scrubbed over a molecular sieve bed. Pressure on the splitless injector was 10 psig and the split ratio was 50 : 1. Other experimental parameters for the GC included: initial temperature, 30 °C; initial time, 5 min; program rate 15 °C min^{-1}; final temperature, 200 °C; final time, 1 min. The FAIMS detector (see Fig. 1) was equipped with a radioactive source (^{63}Ni) of effective activity from 0.6 to 1 mCi. Air was provided as drift gas to the drift tube at 1–2 l min^{-1} using a model 737 Addco Pure Air generator (Miami, FL). The drift gas was further purified over a 5 Å molecular sieve bed (10 cm diameter × 0.6 m long) and heated to 70 °C to warm the drift tube. The drift tube was placed against one side of an aluminium box which also included the amplifier and electronic control circuit and was connected to the GC using a 5 cm section of capillary column. Drift gas carried column effluent through the ion source region where sample vapors were ionized and carried through the gap (0.5 mm) between two flat separating electrodes (5 × 15 mm). Two electric fields were applied to the drift tube: a non-symmetric waveform high frequency (1.3 MHz) with strong (20 kV cm^{-1} *p–p* amplitude) electric field (voltage of 1000 V for plate distance of 0.5 mm) and weak dc field (−360 V cm^{-1} to +80 V cm^{-1}) of compensation voltage (−18 to +4 V_{dc}). When the compensation voltage is slowly swept, the different species of ions will pass through the drift tube, between the plates, and will be recorded at the detector, resulting in a scan with each ion species corresponding to a particular compensation voltage.[11–13] The compensation voltage was scanned with a period of 1 s and 5–8 mobility scans could be obtained over the elution profile of a GC peak where peak widths at baseline were ~5–10 s each. The signal was processed using a National Instruments board (Model 6024E) to digitize and store the scans; specialized software was used to display the results as spectra in topographic plots and graphs of ion intensity *versus* time. Instrumentation for the combined planar FAIMS with a tandem mass spectrometer has been described in detail.[15]

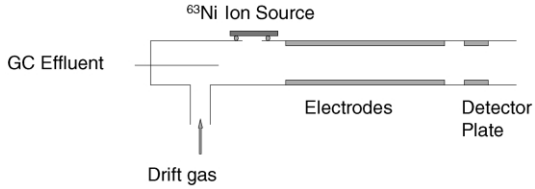

Fig. 1 Flow schematic for PFIMS drift tube as GC detector with capillary column.

Chemicals and solutions

Ketones in the homologous series from butanone to decanone were obtained in analytical grade from various manufacturers and were used as received. A stock solution of the ketones at ~1 mg ml^{-1} in methylene chloride solvent was prepared and used in preparing regularly working solutions. Working solutions were prepared through serial dilutions in methylene chloride. Solutions were stored at −5 °C between analyses. In these studies, working solutions were analyzed in triplicate by GC/FID or GC/PFAIMS.

Procedures

In both GC/FID and GC/PFAIMS studies, samples of 1 µl were introduced to the injection port with a splitless time of 0.75 min. After the start of the measurement, all processes of instrument control and data acquisition were automated. When a measurement was completed, data files were prepared using commercially available spreadsheets. Compensation voltages were determined at peak maxima. Ion identifications were made using a PFAIMS-mass spectrometer which was provided using a continuous flow of vapor with a single ketone. The vapor stream was created using a diffusion tube generator and vapor levels were adjusted with dilution and split flows so the ion distributions were similar to those obtained in GC/PFAIMS studies. The entire PFIMS apparatus including drift tube and electronics was floated so ions would flow from the drift tube through the vacuum interface pinhole to the quadrupole mass spectrometer. Values for compensation voltages were adjusted and kept constant to permit ions from only one peak in the mobility scan to enter the mass spectrometer.[15] Low ion intensity in the mass spectrometer necessitated ~500 averaged scans from 10 to 400 u at 0.1 u s^{-1} to obtain a single mass spectrum.

Results and discussion

Chromatograms and orthogonal information from a PFAIMS detector

The results from a gas chromatographic separation of ketones in a working solution using the micro-machined PFAIMS drift

tube as a detector are shown in Fig. 2 as a topographic plot of retention time *versus* mobility scans. Mobility scans from compensation voltage of −15 to +2.5 V_{dc} (*x*-axis) were obtained every second throughout the elution time from 0 to 900 s (*y*-axis) where with the third dimension (*z*-axis) of the topographic plot is ion intensity. Several key features in this plot include the reactant ion peak at −7.5 V which appears as an intense (~3 V max) peak (marked with dotted white line) throughout the chromatographic elution profile, except when a chemical eluted from the column. This is especially noticeable when the solvent peak eluted at 120–210 s and during the elution of ketones at retention intervals of about 100 s as labeled in Fig. 2 and given in Table 1.

The principal reactant ion peak (RIP) with a ^{63}Ni-based ion source, in air at ambient pressure, is $H^+(H_2O)_n$ (at −7.5 V) and a second, minor RIP was observed at −12 V compensation voltage. This ion was mass identified as ($NH_4^+(H_2O)_n$). When a ketone is introduced into the ion source of the PFAIMS, gas phase ion molecule reactions occur and two product peaks simultaneously appeared in PFAIMS spectra with the same retention time but with different compensation voltages. The relationship of the ion distributions throughout a GC elution profile is shown in Fig. 3 for pentanone. During the elution of a peak, the intensity of a product ions peak grows with a corresponding decrease in intensity for the RIP until a maximum for the GC elution profile is reached. After this, the product ion peak declines in intensity and the RIP peak increases in intensity eventually reaching the original intensity.

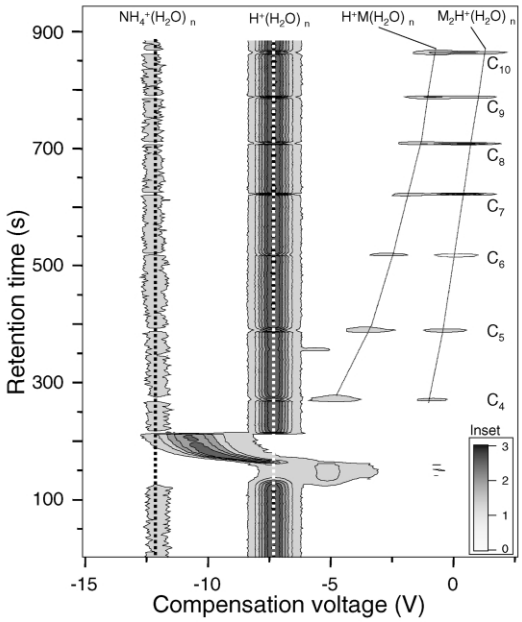

Fig. 2 Topographic plot from GC/PFAIMS analysis of mixture of ketones with mass loading of 3 ng per ketone. The inset shows the shading scale for signal voltage.

This relationship between vapor concentration and ion identity is well-known for techniques employing atmospheric pressure chemical ionization (APCI) and can be explained by the formation of a protonated monomer from reactant ions as shown in eqn. (1).

$$\underset{\text{Reactant ion}}{H^+(H_2O)_n} + \underset{\text{Ketone molecule}}{M} \rightleftharpoons \underset{\text{Protonated monomer}}{MH^+(H_2O)_{n-x}} + \underset{\text{Water molecule}}{xH_2O} \quad (1)$$

Protonated monomers were observed for each ketone and appeared in the mobility scans at compensation voltages from −5.24 to −1.1 V. A proportional dependence between ion mass and compensation voltage is suggested in Fig. 2 and is discussed below. At high mass loadings (or at the maximum of an elution profile for a chromatographic peak), a second ion can be seen in the mobility scans as shown in Figs. 2 and 3. These ions are created through concentration dependent reactions as shown in eqn. (2):

$$\underset{\text{Protonated monomer}}{H^+(H_2O)_n} + \underset{\text{Ketone molecule}}{M} \rightleftharpoons \underset{\text{Proton bound dimer}}{MH^+(H_2O)_{n-x}} + \underset{\text{Water molecule}}{xH_2O} \quad (2)$$

This ion, the proton bound dimer, was observed for all ketones in the PFAIMS drift tube at comparatively high concentrations of sample vapors. The proton bound dimers are marked with dotted lines in Fig. 2. The identities of these ions were also confirmed using a PFAIMS drift tube coupled to a tandem mass spectrometer[15] and the MS results are summarized in Table 1.

The trend toward displacement away from the RIP (+ polarity compensation voltage here) with increasing ion mass was observed for both protonated monomers and proton bound dimers. This trend for the protonated monomers suggests that each ion has a characteristic mobility dependence and there exists a mass dependence for compensation voltage which has not yet been described. For example, the compensation voltage changed from −5.24 V to −1.1 V for compounds ranging from butanone to decanone for a mass difference of about 84 u for the respective product ions of the kind $MH^+(H_2O)_n$. The proton bound dimers also showed a mass dependence though the change in compensation voltage with mass was not as pronounced as that for the protonated monomers. The change in compensation voltage for the proton bound dimers of these ketones was only −1.46 to +0.21 V. Thus, the relative effect of adding a second ketone molecule to the ion cluster is increasingly less important to compensation voltage with increases in molar mass. These differences and their significance are under study and should result eventually in a comprehensive understanding of the meaning of compensation voltages and the relationship to ion structure.[16] Notable in the figures is the stability of the reactant ion peak. Although reactant ions are poor as a chemical standards between instruments, the reactant ion peak here was stable at −7.5 V throughout all measurements and was regarded as a reference internal to each experiment.

Table 1 Experimental findings from GC/PFAIMS and PFAIMS/MS measurements for ketones

	Butanone	Pentanone	Hexanone	Heptanone	Octanone	Nonanone	Decanone
Retention time/s	270	388	517	622	707	786	862
Protonated monomer							
Ion identity	$C_4H_8OH^+$	$C_5H_{10}OH^+$	$C_6H_{12}OH^+$	$C_7H_{14}OH^+$	$C_8H_{16}OH^+$	$C_9H_{18}OH^+$	$C_{10}H_{20}OH^+$
Compensation voltage/V	−5.24	−4.01	−3.13	−2.424	−1.8	−1.36	−1.1
(*m*/*z*)/u	73	87	101	115	129	143	157
Proton bound dimer[a]							
Ion identity	$(C_4H_8O)_2H^+$	$(C_5H_{10}O)_2H^+$	$(C_6H_{12}O)_2H^+$	$(C_7H_{14}O)_2H^+$	$(C_8H_{16}O)_2H^+$	$(C_9H_{18}O)_2H^+$	$(C_{10}H_{20}O)_2H^+$
Compensation voltage/V	−1.46	−1.01	−0.57	−0.31	0.04	0.12	0.21
(*m*/*z*)/u	145	173	201	229	257	285	313

[a] Could be minor amounts of higher order cluster under the mobility peak.

An added analytical importance of the results in Fig. 2 is that mobility scans provide orthogonal information during a chromatographic separation and this increases the level of confidence in chemical identification by GC analysis. The combination of retention time and peak values of compensation voltage are characteristic of ions from each ketone. Another view of the mobility scans, obtained throughout the elution profile, is shown in Fig. 4 as plots of ion intensity *versus* compensation voltage. In these plots, spectra from throughout the elution profile for a ketone are shown as a composite in a single frame. The spectra show reactant ion peaks (shaded) and product ions (as labeled): protonated monomers (PM) and proton bound dimer (PBD). The concentration dependence in these results is identical to that of traditional mobility spectrometers, namely, charge is displaced to the protonated monomer and the proton bound dimer sequentially as vapor levels increase. This common behavior suggests that the high field environment is not disruptive to ion behavior as understood from low field experiments. Similar patterns were observed for nonanone (not shown). This is a first disclosure of the concentration dependence of mobility scans from PFAIMS and the findings suggest that the well-established understandings of ion behavior can be extended to PFAIMS instruments. These findings suggest the importance of creating a spectral library of mobility scans for future analytical uses.

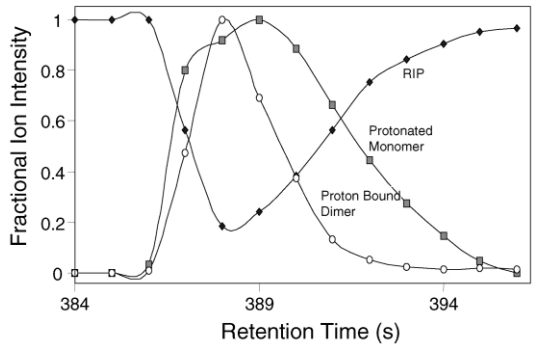

Fig. 3 Plot of intensities of peaks (as fractional amounts of individual ion species) in a mobility scan throughout the GC elution profile for pentanone.

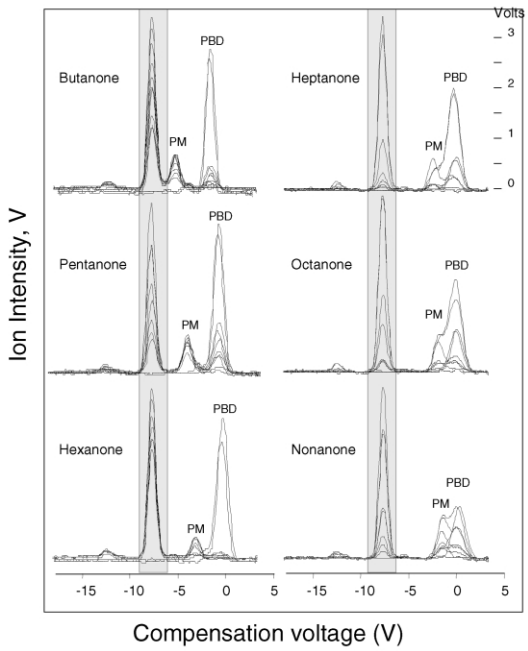

Fig. 4 Composites of PFAIMS spectra for ketones obtained from a range of sample vapor concentrations. Peaks can be seen for the reactant ion peak (shaded), the protonated monomer (PM) and the protein bound dimer (PBD) for ketones as labeled.

Chromatographic performance

In addition to the topographic display of analytical results, the use of product ion intensity can allow analytical performance to be simplified and compared directly with that for an FID.[17] This is shown in Table 2 and Fig. 5 where chromatographic profiles are shown in a traditional 2D plot. Such plots can be generated by summarizing the intensity for all protonated monomers and

Table 2 Comparision of chromatographic performance with FID and PFAIMS. Chromatographic terms measured were: number of theoretical plates (N), plate height of a theoretical plate (H), and the skew ratio (η)

Compound	N	H/mm	η
GC FID—			
Butanone	3.62×10^4	6.91×10^{-1}	0.93
Pentanone	5.20×10^4	4.81×10^{-1}	0.93
Hexanone	1.83×10^5	1.37×10^{-1}	0.91
Heptanone	2.40×10^5	1.04×10^{-1}	0.83
Octanone	2.33×10^5	1.07×10^{-1}	0.86
Nonanone	3.64×10^5	6.87×10^{-2}	0.77
Decanone	3.78×10^5	6.61×10^{-2}	0.85
Average	2.12×10^5	1.18×10^{-1}	0.87
Relative standard deviation (%)	1.35×10^5	1.85×10^{-1}	
GC PFIMS—			
Butanone	2.89×10^4	8.65×10^{-1}	0.30
Pentanone	3.73×10^4	6.70×10^{-1}	0.63
Hexanone	1.11×10^5	2.25×10^{-1}	0.33
Heptanone	2.32×10^5	1.08×10^{-1}	0.43
Octanone	1.70×10^5	1.47×10^{-1}	0.43
Nonanone	2.45×10^5	1.02×10^{-1}	0.88
decanone	2.51×10^5	9.96×10^{-2}	0.71
Average	1.53×10^5	1.63×10^{-1}	0.53
Relative standard deviation (%)	9.59×10^4	2.61×10^{-1}	

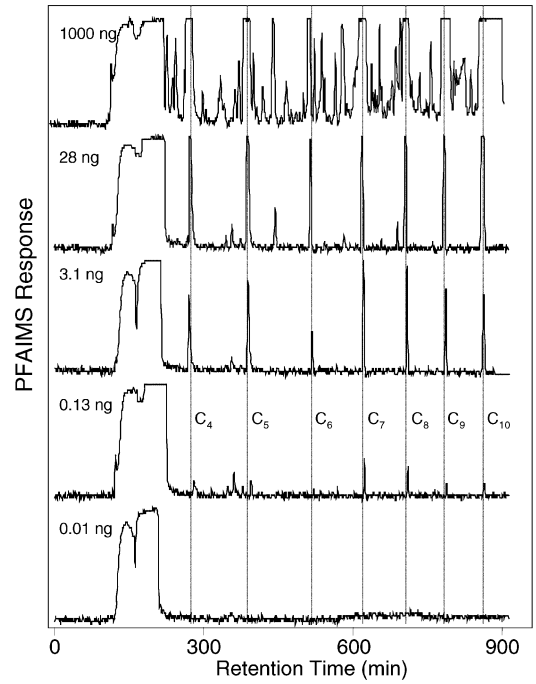

Fig. 5 Chromatograms from GC/PFAIMS characterization of a mixture of ketones at several concentrations; individual mass loadings are shown. The intensity axis is inverted intensity from the reactant ion peak.[17]

proton bound dimer ions in every spectrum and plotting intensity *versus* retention time. A second and convenient manner to create these plots came through recording and continuously inverting the intensity of the RIP peak throughout the GC elution time. These methods provide qualitatively identical results. The effect of amount of sample is shown in Fig. 5 as chromatograms from the GC separation of the ketone mixture with the micro-machined PFAIMS detector for several mass loadings. The amounts of ketones ranged from below the detection limit (bottom trace) to severe overload in response (top trace). The mass values for these corresponded to 10 pg to 1000 ng, respectively. In each chromatogram, a solvent peak can be observed at 120–210 s and seven ketones peaks from butanone to decanone at regular intervals as expected for a homologous series and a temperature programmed oven. The appearance of the chromatograms shows peak shape, throughout the range of mass loading, without obvious tailing or peak distortions. However, a quantitative analysis of chromatographic efficiency and peak shape from the FID and the PFAIMS detector is given in Table 2. The efficiencies ranged from plate heights of 0.06 to 0.2 mm for the FID with a mean of 0.19 mm and 0.1–0.2 mm for the PFAIMS with a mean of 0.26 mm. In short, extra column broadening due to the PFAIMS detector was 36% larger than that for the FID. Presumably, the increased surface area and turbulence caused some extra-column broadening. This was also seen in peak shape, expressed as the skew ratio in Table 2, where the PFAIMS performance was worse than the FID. These numbers should be considered preliminary since little or no effort was given to optimization of the FAIMS as GC detector, rather a simple flow connection was made. In terms of function, this approach allowed a convenient transition between these two detectors.

Quantitative response characteristics

As with nearly all other mobility spectrometers, the radioactive ion source for this analyzer continuously emits beta particles in the same manner as an electron capture detector. This source has served in conventional mobility spectrometry for decades but is accompanied by a set of limitations. The response of such a source is commonly considered linear from the limit of detection (LOD) to a point of saturation not much more than 10× above the LOD. This is true here also and is linked to the ion source rather than the drift tube. The PFAIMS response exhibited narrow linear ranges for all ketones and was saturated in peak height by 28 ng; further increases in mass loading of sample caused only peak broadening. Nevertheless, response on the detector was proportional to mass below ~30 ng and comparison of response between the FID and the PFAIMS detector is shown in Fig. 6. Proportional, though not linear, analytical response could be obtained over four orders of magnitude for the PFAIMS; by comparison, the FID showed additional range of 10–100 in linear response that was not observed with the PFAIMS. The limit of detection was 1.3 ng for the PFAIMS and 8 ng for the FID or an improvement of nearly 7× that of an FID. However, sensitivity as $\Delta R/\Delta$mass for the PFAIMS was not as steep as that for the FID by more than 4×. This limitation is attributable to the ion source and not to the principles of gas phase ion characterization by ion mobility.

Precision (reproducibility) from five replicate determinations of the ketone solutions by GC/FID and GC/PFAIMS are presented in Table 3. The solution for this study contained 28 ng of each ketone. The average value for precision from the determination of all ketones was 5.8% for the FID and 5.9% for the PFAIMS detector. These results demonstrate that repeatability for the PFAIMS is as good as the FID and the additional ion characterization contributes no measurable increase in variance.

Conclusions

The planar micro-scale drift tube for ion mobility spectrometry with high electric fields and asymmetric waveforms (PFAIMS) adds chemical information as the mobility scans to a chromatographic separation. This gives value to the analytical measurement beyond that of an FID and such orthogonal information to GC separations should add confidence to chemical identifications *versus* only retention (time, volume, index). The limits of detection were comparable with those from a commercial FID though extra-column broadening in the PFAIMS was worse than with the FID. However, this is a first generation instrument lacking optimization and refinements. Other aspects of performance, including the influence of co-eluting components on quantitative determinations, are under study. In addition, the influence of performance from drift tube parameters have not

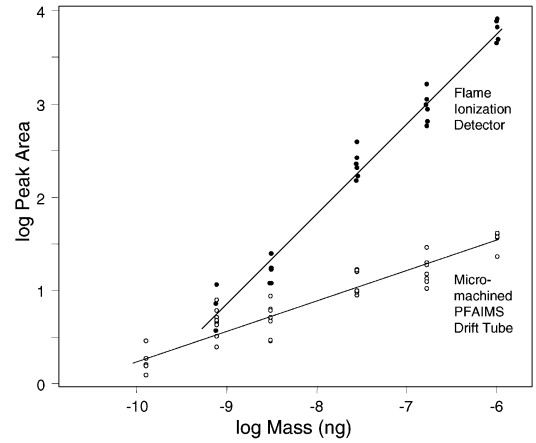

Fig. 6 Average response curves for ketones from GC measurements with the FID and a PFAIMS as detector.

Table 3 Quantitative precision from repeated chromatographic determinations of ketones

	Average peak area	Standard deviation	Standard deviation (%)
GC FID—			
Butanone	65.5	3.7	5.6
Pentanone	122.2	5.7	4.7
Hexanone	29.6	3.2	10.7
Heptanone	196.5	9.7	4.9
Octanone	132.7	7.6	5.8
Nonanone	162.0	8.7	5.4
Decanone	93.5	3.3	3.5
Average			5.8
RF IMS—			
Butanone	3.76	0.24	6.4
Pentanone	5.52	0.26	4.7
Hexanone	2.70	0.10	3.9
Heptanone	2.96	0.16	5.5
Octanone	2.76	0.17	6.2
Nonanone	3.37	0.27	7.9
Decanone	4.55	0.21	4.6
Average			5.9

been thoroughly documented nor have models to link molecular structure to compensation voltage.

Acknowledgements

Support is gratefully acknowledged from the university cooperation grants from Charles Stark Draper Laboratory (Award No. DL-H-516600) and from NASA (Grant No. 00-HEDS-01-110).

References

1 G. A. Eiceman, H. H. Hill, Jr. and J. Gardea-Torresday, *Anal. Chem.*, 2000, **72**, 137R.
2 J. Baumbach and G. A. Eiceman, *Appl. Spectrosc.*, 1999, **53**, 338A.
3 G. A. Eiceman and Z. Karpas, *Ion Mobility Spectrometry*, CRC Press, Boca Raton, FL, 1993.
4 M. A. Baim and H. H. Hill, Jr., *Anal. Chem.*, 1982, **54**, 38.
5 G. A. Eiceman, E. G. Nazarov and J. E. Rodriquez, *Anal. Chim. Acta*, 2001, **433**, 53.
6 S. E. Bell, E. Nazarov, Y.-F. Wang, J. E. Rodriquez and G. A. Eiceman, *Anal. Chem.*, 2000, **72**, 1192.
7 T. Limero, *A Second Generation Volatile Organic Analyzer for the International Space Station*, International Conference On Environmental Systems, July 1999, Denver, CO, Paper 1999-01-2059.
8 J. I. Baumbach, D. Berger, J. W. Leonhardt and D. Klockow, *Int. J. Environ. Anal. Chem.*, 1993, **52**, 189.
9 G. A. Eiceman, B. Tadjikov, E. Krylov, E. G. Nazarov, R. A. Miller, J. Westbrook and P. Funk, *J. Chromatogr., A*, 2001, **917**, 205.
10 R. A. Miller, G. A. Eiceman and E. G. Nazarov, *Sens. Actuators B*, 2000, **67**, 300.
11 R. A. Miller, E. G. Nazarov, G. A. Eiceman and T. A. King, *Sens. Actuators A*, 2001, **91**, 301.
12 http://www.faims.com/main.html.
13 I. A. Buryakov, E. V. Krilov, E. G. Nazarov and U. Kh. Rasulev, *Int. J. Mass Spectrom. Ion Processes*, 1993, **48**, 114.
14 R. E. Ewing, J. A. Stone and G. A. Eiceman, *Int. J. Mass Spectrom.*, 1999, **193**, 57.
15 G. A. Eiceman, E. G. Nazarov and R. A. Miller, *Int. J. Ion Mobility Spectrom.*, 2001, **3**, 15.
16 M. L. Easterling, C. M. Colangelo, R. A. Scott and I. J. Amster, *Anal. Chem.*, 1998, **70**, 2704.
17 F. W. Karasek, H. H. Hill, Jr., S. H. Kim and S. Rokushika, *J. Chromatogr.*, 1977, **135**, 329.